The International Journal of Advanced Manufacturing Technology (2024) 132:4785–4794
https://doi.org/10.1007/s00170-024-13600-0

ORIGINAL ARTICLE

Fabrication of the optical lens on single-crystal germanium surfaces using the laser-assisted diamond turning

Hanheng Du[1,2] · Yidan Wang[3] · Yuhan Li[2] · Yintian Xing[2] · Sen Yin[2] · Suet To[2,4]

Received: 7 November 2023 / Accepted: 9 April 2024 / Published online: 25 April 2024

Abstract

Single-crystal germanium, as an excellent infrared optical material, has been widely applied in X-ray monochromators, night vision systems, and gamma radiation detectors. However, how to obtain high-quality optical lenses on their surfaces still faces challenges due to their hard and brittle properties. To this end, this paper proposes the in situ laser-assisted diamond turning (ILADT) process, which is the combination of a laser heating technique and a single-point diamond turning process. The in situ laser heating technique is employed to enhance the surface quality of the workpiece material, while the single-point diamond turning process is utilized to fabricate optical lenses. Experimental results showed that optical lenses with high surface quality were successfully machined. The profile error is 0.135 μm, indicating the high machining accuracy. The surface roughness Sa of the aspheric lens is 0.909 nm, indicating the high machining quality achieved by the proposed ILADT process. Therefore, this study provides an effective approach for producing high-quality optical lenses on single-crystal germanium surfaces, which holds great promise for future applications in the manufacturing of optical lenses with exceptional quality.

Keywords Optical lens · Single-crystal germanium · Single-point diamond turning · Laser heating · Surface roughness

1 Introduction

The optical lens has the capability of manipulating light and forming images, which has widespread application in digital cameras [1], microscopes [2], projectors [3], eyeglasses [4], and medical imaging [5]. Recently, Apple Inc. announced a very advanced wearable headset device, named Vision Pro, which helps customers enjoy a mixed-reality experience. In this device, a large number of optical lenses are used to create this mixed-reality experience [6]. Therefore, the task of machining optical lenses with spherical or aspheric surfaces, while aiming for high efficiency and high quality, continues to encounter numerous challenges [7, 8].

Lots of research efforts have been devoted to solving this problem and the growing demand for optical lenses. Grinding is a common machining method to shape optical lenses and achieve the desired surface profile [9–11]. After determining the suitable grinding parameters and grinding tools, the rough grinding and fine grinding are sequentially conducted. To reduce the number of machining steps, Kakinuma et al. proposed a chemical action-assisted ultraprecision grinding to create optical glass lenses [10]. Experimental results show this approach provides production efficiency by five times. To improve the machining accuracy of optical aspheric surface micro-lenses on glass BK7, Lee and Baek developed an ultraprecision grinding system based on the factorial design and considering the profile error and surface roughness, the grinding condition was optimized by the design of experiments [11]. Yan et al. proposed an off-spindle-axis spiral grinding method to machine the aspheric

✉ Suet To
sandy.to@polyu.edu.hk

Hanheng Du
duhanheng@outlook.com

1 School of Mechanical Engineering and Automation, Beihang University, Beijing, China

2 State Key Laboratory of Ultra-Precision Machining Technology, Department of Industrial and Systems Engineering, The Hong Kong Polytechnic University, Hong Kong, China

3 State Key Laboratory of High-Performance Precision Manufacturing, Dalian University of Technology, Dalian, China

4 The Hong Kong Polytechnic University Shenzhen Research Institute, Shenzhen, China

microlens array mold inserts on tungsten carbide surfaces. Experimental results showed the form accuracy was below 0.3 μm in peak-to-valley and the surface roughness was below 10 nm in Sa, showing the high machining accuracy and machining quality [12]. To further improve the profile accuracy, some compensation methods were also proposed [9, 13–15]. Ultraprecision polishing is another mechanical method to machine optical lenses [16–18]. Suzuki et al. added the two-axis ultrasonic vibration motion to the polisher, which helps to achieve the high numerical aperture optics [19]. Using this method, the surface roughness Rz of the binderless tungsten carbide can reach 8 nm. Based on this work, Guo et al. developed a magnetostrictive vibrating polisher to further enhance the machining efficiency and machining quality. The surface roughness was decreased to 3.3 nm [20, 21]. Cheung et al. utilized computer-controlled ultraprecision polishing to machine various structured surface patterns [22]. However, ultraprecision grinding, or ultraprecision polishing are usually limited by low material removal rates.

Ultraprecision diamond turning using a natural single-crystal diamond cutting tool become an increasingly popular process [23–26]. As a one-step process, it does not post-processes, which saves the machining time. Fang et al. applied the ultraprecision single-point diamond turning process to a machine conical reflector and established the theoretical relationship between the machined surface quality, machining conditions, and optical defects [27], which provides powerful guidance for selecting appropriate machining conditions. Chen, Li, and Yi proposed a three-dimensional microstructure fabrication method, which combines the reactive ion etching technique and ultraprecision single-point diamond turning. Different from the lithography-based method, this new method can machine continuous three-dimensional features. A sine wave grating and a diffractive optical pattern were successfully machined by this method [28]. Considering the huge requirement of the microlens arrays in advanced infrared (IR) optics, Mukaida and Yan applied slow tool servo diamond turning to fabricate the IR microlens arrays. After experimental investigation, they found amorphization and microfracture occur on a single side of the lens dimple when high tool feed rates were employed [29]. However, the microfracture or micro-crack on the optical lens surfaces has a significant influence on the properties and performance of the optical lens. For example, it can cause light to scatter as it interacts with the irregularities of the crack edges, and the scattered light can result in a loss of contrast, reduced image clarity, and decreased overall brightness. Micro-cracks can affect the reflection and refraction of light, which reduces optical efficiency.

Germanium (Ge) is a widely used optical material with excellent optical properties, such as a high transparency range, high refractive index in the IR range, low dispersion, and good thermal stability [30–34]. But Ge is a brittle material with low fracture toughness, which makes it prone to cause micro-cracks or other defects. To mitigate or even avoid the influence of micro-cracks or microfracture, a novel machining method needs to be proposed to enhance the surface quality of optical lenses.

In this study, an in situ laser-assisted diamond turning process is proposed in the machining of optical lenses with excellent surface quality, making it valuable in industries such as aerospace, defense, and telecommunications. Machining experiments were performed to validate the effectiveness of the in situ laser-assisted diamond turning process. Additionally, the machined optical lenses were characterized, and their surface quality and Raman spectroscopy were analyzed in this paper.

2 Methods

2.1 Machining principle of the ILADT process

In situ laser-assisted diamond turning (ILADT) is a new ultraprecision machining process, which can be applied in machining complex optical components with high surface quality [35], especially optical lenses. Figure 1 illustrates the hardware setup and working principle of the ILADT process. This process combines the working principle of single-point diamond turning, which is a form of ultraprecision machining using a natural single-crystal diamond (SCD) cutting tool, with the application of laser heating to enhance the machinability of the hard and brittle material. The sample is fixed on the C-axis of the ultraprecision lathe using a home-developed fixture. The ultraprecision lathe allows for the ultraprecision control of the position and orientation of the sample during machining. A SCD cutting tool is mounted on the laser module, which is installed on the Z-axis of the ultraprecision lathe. The SCD cutting tool has a very sharp cutting edge, normally less than 100 nm, which satisfies the surface finish and accuracy requirements of optical lenses. In the machining of the optical lenses, the cutting tool will contact with the rotating sample, and the desired shape is achieved by the combination of the workpiece rotation and cutting tool translation. In the ILADT process, a laser beam is directed onto the sample surface to heat and soften the workpiece material at the cutting zone after passing through the SCD cutting tool, as shown in Fig. 1. The laser assistance reduces the cutting forces required for material removal and then improves surface quality. Therefore, the laser power, spindle speed (which controls the workpiece rotation), and feed rate (which controls the cutting tool translation) should be carefully determined to ensure optimal surface quality.

In general, the optical lens with the aspheric surface can be mathematically described by an aspheric equation. The

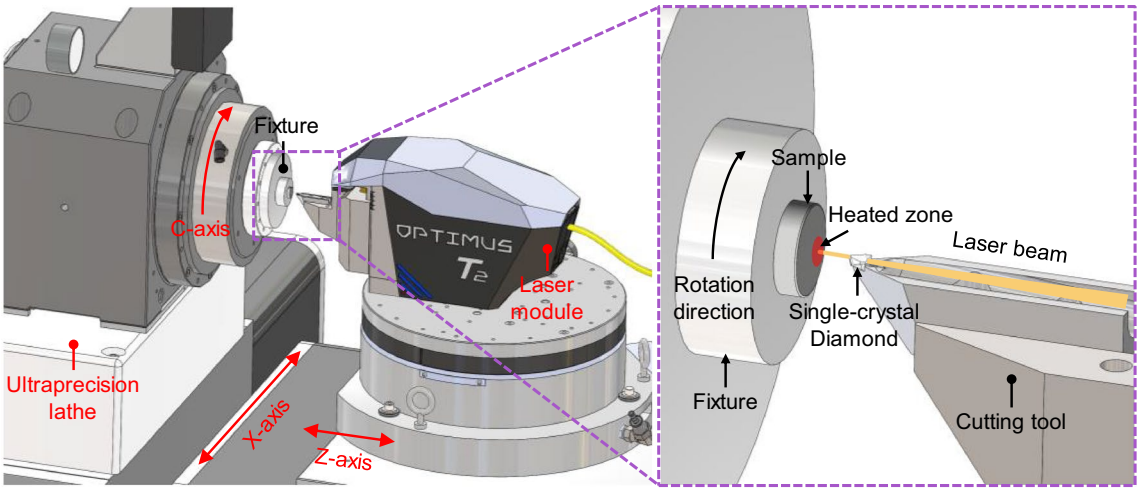

Fig. 1 Working principle of the ILADT process

aspheric equation represents the deviation of the lens surface from a perfect sphere, allowing for more complex surface profiles that can correct for various optical aberrations. The general form of the aspheric equation in the Z direction is:

$$z(p) = \frac{Cp^2}{1 + \sqrt{1 - (K+1)C^2p^2}} + \sum_{i=1}^{n} A_i p^i \tag{1}$$

$$p = \sqrt{x^2 + y^2} \tag{2}$$

where x and y are the Cartesian coordinates in the lens plane. $C = 1/R$, and R represents the radius of curvature of the spherical surface (positive for convex surfaces and negative for concave surfaces). p denotes the distance from the optic axis Z. K refers to the conic constant, which determines the shape of the surface. A_i is the aspheric deformation constant [36, 37].

2.2 Experimental setup of the optical lens

Figure 2 shows the experimental setup when machining optical lenses. This hardware system can be divided into two main parts: the ultraprecision lathe and the laser control module. The ultraprecision lathe with three axes is the 450 UPL of the Moore Tool Company, USA. This lathe provides ultrahigh control and feedback systems to monitor and adjust the feed rate and spindle speed during machining, which ensures the creation of complex geometries and nanoscale surface quality. The laser control module is the Optimus T_2 of the Micro-LAM. Inc., USA, which is fixed on the Z-axis

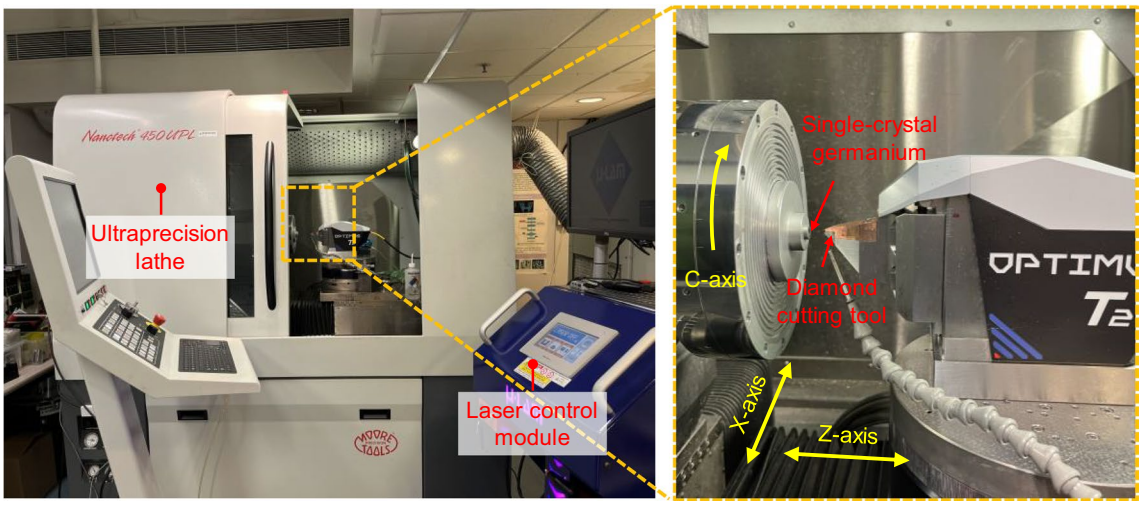

Fig. 2 Experimental setup of machining optical lenses on single-crystal germanium surfaces

Table 1 Geometrical parameters of the machined optical lens

R (mm)	K	Diameter (mm)	A_i
5	−0.1	5	0

Table 2 Geometrical parameters of the cutting tool and machining parameters

Cutting tool parameters		Machining parameters			
Radius (mm)	0.497	Roughing machining		Finishing machining	
Flank angle	15°	Feed rate (μm/rev)	2	Feed rate (μm/rev)	0.8
Rake angle	−35°	Spindle speed (RPM)	83	Spindle speed (RPM)	83

of the ultraprecision lathe. Its control and laser delivery devices ensure that the stable laser beam can be directed onto the cutting zone of the sample. The laser source is the Nd: YAG laser in this study, and the laser power is set at 1.75 W to induce localized heating and soften the sample surface. The single-crystal germanium, as the sample, is fixed on the C-axis of the ultraprecision lathe, as depicted in Fig. 2.

Table 1 lists the geometrical parameters of the machined optical lenses. The selection of the cutting tool is crucial for achieving good machining results. Different from the traditional single-point diamond cutting, the ILADT process possesses a cutting tool with a negative rake angle according to the requirements of the laser beam and workpiece material. Table 2 describes the detailed geometrical specifications of the used cutting tool. The diameter of the single-crystal germanium (111) is 10 mm, and the optical lens was machined on the center of the sample. The spindle speed is set as 83 revolutions per minute, and other parameters of the roughing machining and finishing machining are summarized in Table 2.

Following the machining experiments, the samples were subjected to cleaning using an ultrasonic cleaner. A white light interferometer (Nexview™, Zygo Corp., USA) was used to characterize their surface roughness. The profile of the machined optical lenses was characterized by contact form measurement equipment (Form TalySurf PGI 1240, Taylor Hobson, England).

3 Results and discussion

3.1 Superiority of the ILADT process

Considering that single-crystal germanium is a typical hard and brittle material, a sculpturing method was conducted to determine its critical depth-of-cutting. This method can be found in Ref. [38, 39]. In the experiments, the sample was fixed on the spindle. The SCD cutting tool is fed at a consistent cutting speed, while simultaneously, the depth of cut progressively increases along the Z-axis direction of the ultraprecision lathe. To show the superiority of the proposed ILADT process, the traditional single-point diamond turning (SPDT) was also applied to carry out the sculpturing experiment. Figure 3 shows the results of the sculpturing experiments on the topography and cross-sectional profile of microgrooves when using the proposed ILADT process and traditional SPDT. From the cross-sectional profile that goes through the center of the microgroove, it can be found that the critical depth-of-cuttings of the single-crystal germanium are 130.19 nm and 79.32 nm, respectively. The information provided states that the proposed ILADT process improves the critical depth-of-cuttings by 64.1%, which shows its superiority. This improvement also leads to improved machining capabilities and potentially enabling the production of more advanced optical components.

Before generating an optical lens on the single-crystal germanium surfaces, the mirror surface needs to be machined, and their surface roughness is characterized by applying the white light interferometer. Figure 4 shows the measurement results. The surface roughness parameter Ra represents the average value of absolute surface height deviations from the mean line over the evaluation length. The surface roughness parameter Rz represents the vertical distance between the highest peak and the lowest valley. Sa is 0.478 nm when using the proposed ILADT process while that is 1.035 nm when using the traditional SPDT process. The values of Sz are 5.354 nm and 15.048 nm, respectively. It can be found that Sa and Sz are decreased by 53.8% and 64.4%, respectively, showing the effectiveness of the proposed ILADT process in enhancing the machined surface quality of the single-crystal germanium.

3.2 Characterization of optical lenses

After cleaning by an ultrasonic cleaner, the machined samples can be obtained. Figure 5 shows photographs of the machined optical lens when using the traditional SPDT process and the ILADT process, which are captured by the high-resolution digital camera.

Figure 6 displays the three-dimensional (3D) topography, cross-sectional profile, and profile error of the machined optical lenses by the proposed ILADT process and traditional SPDT process. The 3D topography was obtained by the white light interferometer. Because of the limited measurement range of the white light interferometer, part of the machined optical lens can be only captured. In order to obtain the whole profile of the machined optical lens, a contact metrology method was applied using the

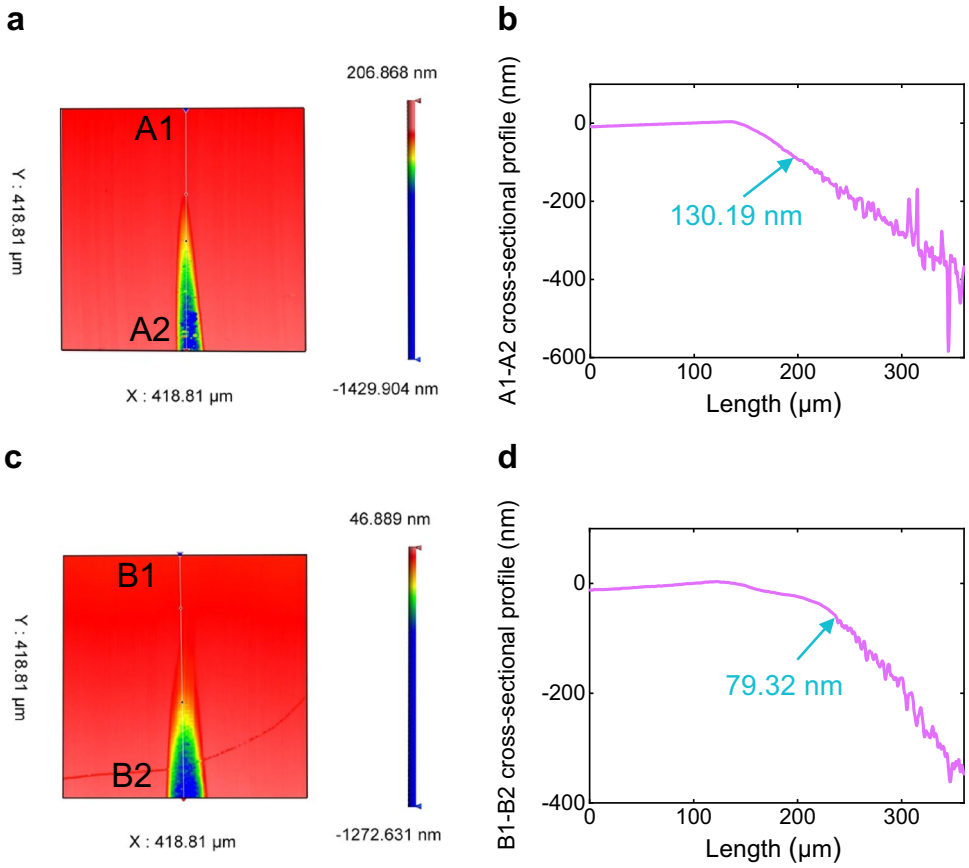

Fig. 3 Microgrooves machined by the sculpturing method. **a** and **b** show its topography and cross-sectional profile using the ILADT process. **c** and **d** show its topography and cross-sectional profile using the traditional SPDT process

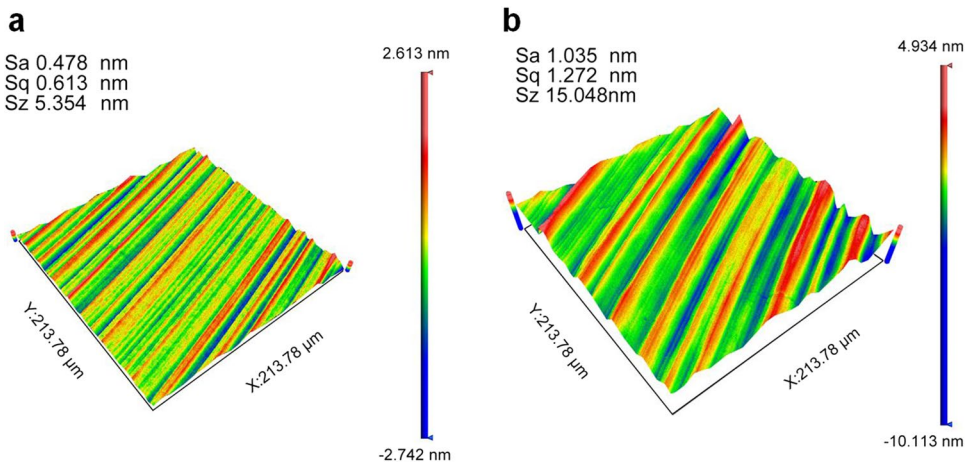

Fig. 4 The surface quality of the mirror surface when **a** using the ILADT process and **b** using the traditional SPDT process

form measurement equipment (Form TalySurf PGI 1240, Taylor Hobson, England). The measured cross-sectional profile (passes through the center of the optical lens) and profile error (the difference between the designed profile and the measured cross-sectional profile) were also plotted. The profile error is 0.135 μm when using the ILADT process and that is 0.209 μm when using the SPDT process. It can be also found that the two cross-sectional profiles are very close. This phenomenon is verified by the SEM images of the SCD cutting tool after machining, as shown in Fig. 7. The cutting edges of the two SCD cutting tools remain intact (no tool wear). Besides, the machining parameters and machining settings are totally the same. Therefore, there is no obvious difference in the cross-sectional profiles when using the ILADT process and the traditional SPDT process.

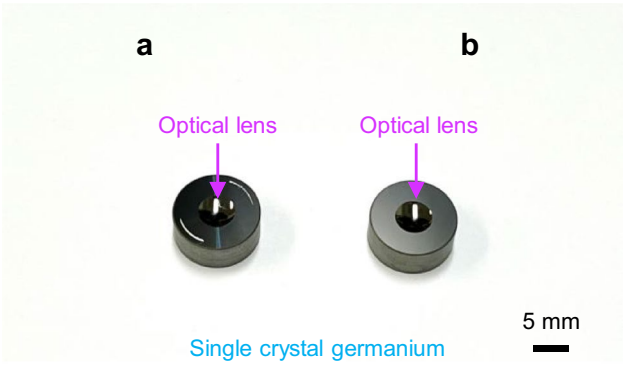

Fig. 5 Photographs of the optical lens when **a** using the traditional SPDT process and **b** using the ILADT process

3.3 Analysis of the surface quality

In addition to the cross-sectional profile, the surface quality is more important, which directly impacts the working performance of the optical lens [40, 41]. The 213.78 μm × 213.78 μm areas of the machined optical lens were randomly extracted. Their surface quality is quantitatively characterized by the white light interferometer, as depicted in Fig. 8. When applying the ILADT process, the surface roughness Sa and Sz are 0.909 nm and 10.560 nm. If using the traditional SPDT process, they are 1.328 nm and 17.080 nm. It can be found that the proposed ILADT process decreases the surface roughness Sa and Sz by 31.6% and 38.2%, demonstrating the superiority and effectiveness of the proposed ILADT process in generating high-quality optical lenses.

Finite element simulation is an efficient tool for comprehending the proposed ILADT process. Figure 9 shows the simulation results on the contour plot depicting the von Mises equivalent stress, obtained through the utilization of the ABAQUS software. It can be found from the visualization

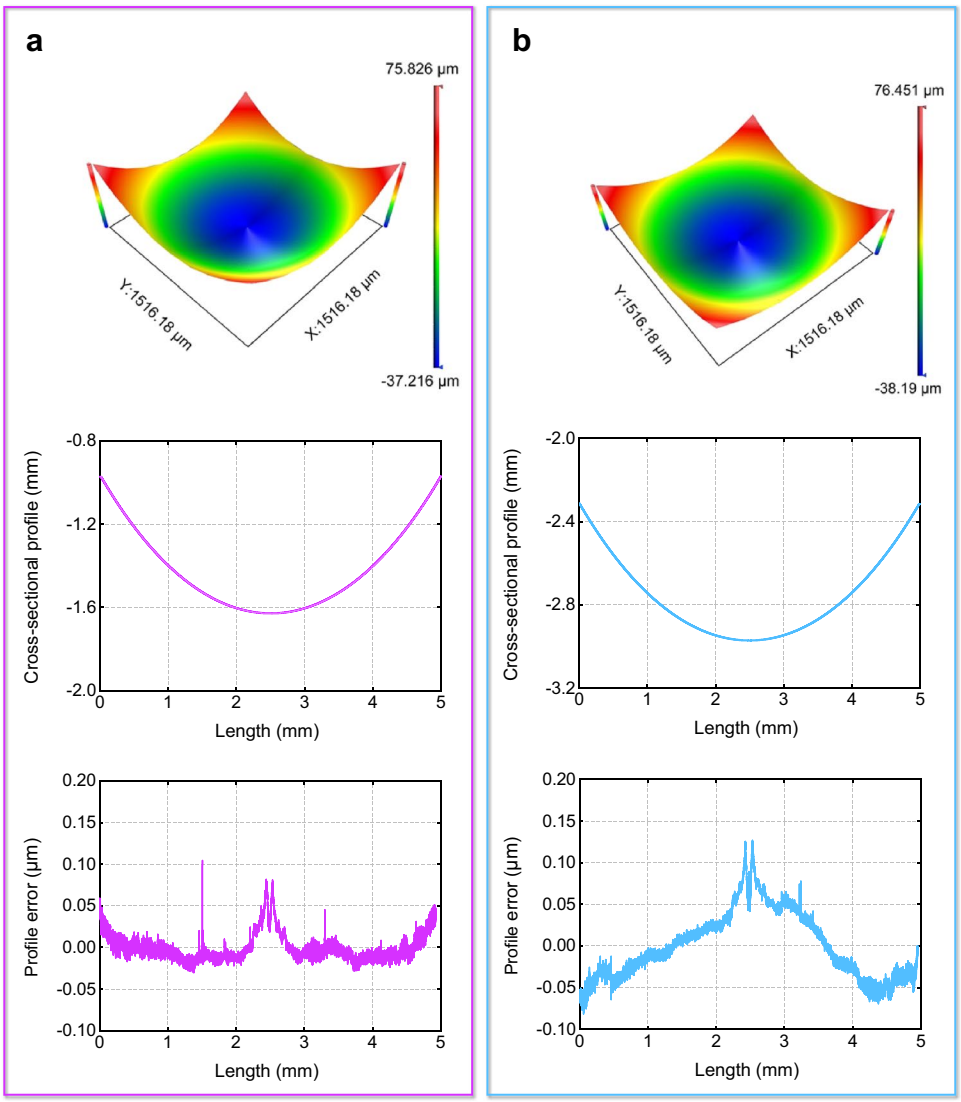

Fig. 6 3D topography, cross-sectional profile, and profile error of optical lens. **a** Using ILADT process and **b** using the traditional SPDT process

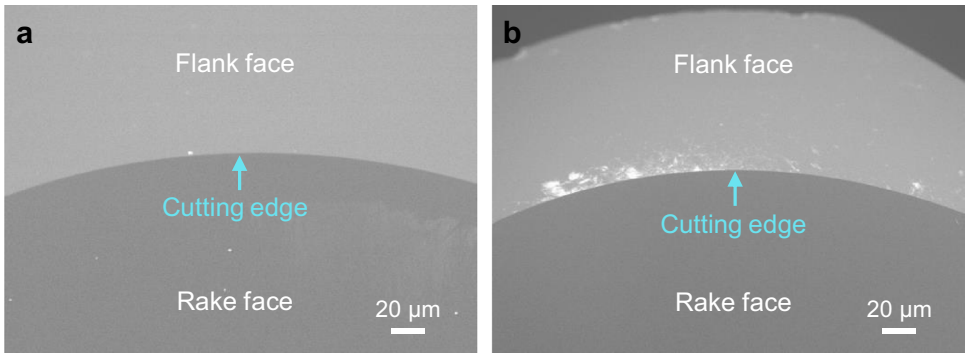

Fig. 7 SEM images of the SCD cutting tools after machining. **a** ILADT process and **b** traditional SPDT process

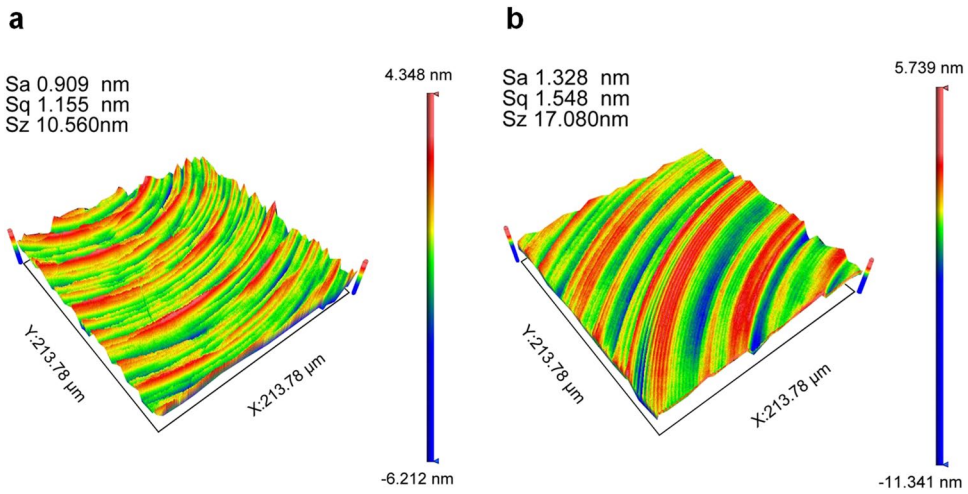

Fig. 8 Surface quality of machined optical lenses by using **a** the ILADT process and **b** the traditional SPDT process

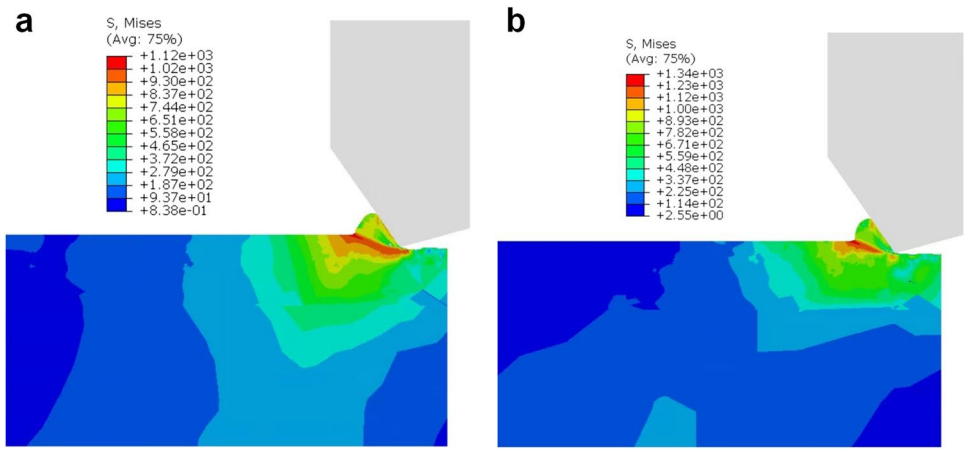

Fig. 9 Contour plot of the von Mises equivalent stress. **a** The ILADT process and **b** the traditional SPDT process

analysis that, in comparison to the traditional SPDT process, the proposed ILADT process obviously reduces the von Mises equivalent stress. Specifically, in the shear zone, the von Mises equivalent stress is observed to decrease by 16.4% when employing the ILADT process. This reduction in von Mises equivalent stress helps to improve the machining quality.

Considering that Raman spectroscopy, as a non-destructive and non-contact technique, is a powerful tool for analyzing structural defects and stresses introduced by the machining processes [42, 43], Raman spectroscopy was also used to provide valuable insights into the variations of the material by measuring Raman peaks. Figure 10 depicts the Raman spectrum of machined optical lenses by using the ILADT process and traditional SPDT process. Raman peak observed at approximately 303 cm^{-1} is attributed to the longitudinal optical (LO) phonon mode, which is linked with

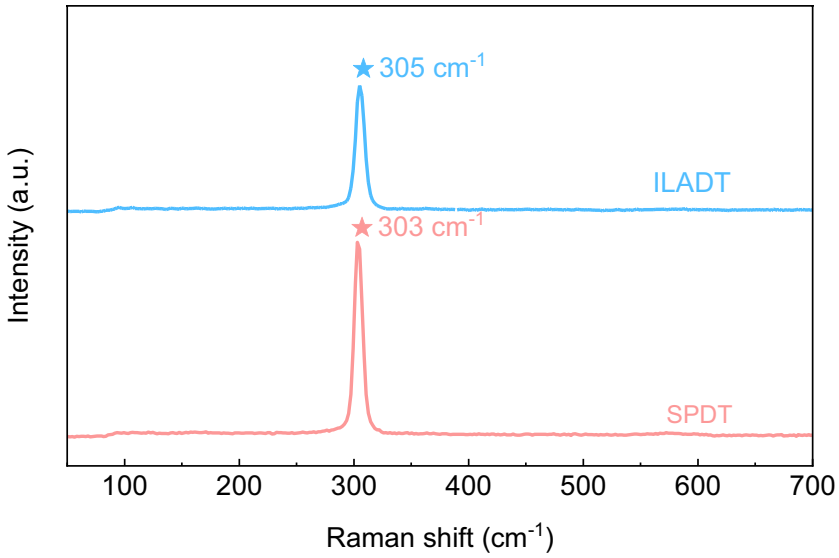

Fig. 10 Raman spectrum of machined optical lenses by using the ILADT process and traditional SPDT process

the Ge–Ge bonds [44]. The significant shift of the Raman peaks, from 303 to 305 cm^{-1}, indicates the introduction of a minor compressive stress facilitated by laser heating. The minor compressive stress can enhance the mechanical properties of the material because it helps to stabilize the crystal structure and reduce the likelihood of dislocation movement [45, 46]. Additionally, compressive stress can effectively reduce the occurrence of surface defects in machined optical lenses on the surfaces of single-crystal germanium. Machining processes can introduce surface defects [47], including scratches and cracks, which can negatively impact the performance of optical lenses. The minor compressive stress plays a crucial role in mitigating the formation and propagation of these defects, thereby enhancing the surface quality and integrity of the machined optical lenses. This is particularly important in optical applications where surface quality is crucial for achieving high optical transmission and minimizing scattering or absorption losses. This also explains the reason why the ILADT process can decrease the surface roughness of machined samples. The benefits help to optimize the performance and reliability of optical lenses in various applications, including MEMS, optical devices, semiconductor devices, and thermal management systems.

4 Conclusions

In this study, an in situ laser-assisted diamond turning (ILADT) process is employed to machine optical lenses with high surface quality and high machining accuracy on surfaces of the single-crystal germanium, which is known for its hardness and brittleness. The ILADT process combines an in situ laser heating technique and a single-point diamond turning process, which helps to enhance the surface quality and remove the workpiece material. Therefore, the ILADT process can merge the benefits of the in situ laser heating technique and the single-point diamond turning process, which facilitates the high-quality machining of optical lenses.

ILADT process fabricated optical aspheric lenses on the single-crystal germanium surfaces, demonstrating high machining accuracy and machining quality. The measured profile error was found to be less than 0.2 μm, while the surface roughness (Sa) was less than 1 nm. Raman spectroscopy analysis revealed that the introduction of minor compressive stress through laser heating played a significant role in improving machining quality. Therefore, this study offers a valuable technology in the realm of fabricating high-quality optical lenses on single-crystal germanium surfaces. This technology holds great potential for the manufacturing of optical components with intricate geometries, precise tolerances, and exceptional surface finishes in the field of optical engineering.

Author contribution Hanheng Du: conceptualization, methodology, validation, formal analysis, investigation, visualization, writing—original draft, writing—review and editing. Yidan Wang: writing—review and editing. Yuhan Li: investigation. Yintian Xing: writing—review and editing. Sen Yin: writing—review and editing. Suet To: resources, supervision, project administration, funding acquisition.

Funding Open access funding provided by The Hong Kong Polytechnic University This work was supported by the Research Grants Council of the Hong Kong Special Administrative Region, China (Project No.: PolyU 15221322), the National Natural Science Foundation of China (Project No.: U19A20104), the Shenzhen Science and Technology Program (Project No.: JCYJ20210324131214039), and State Key Laboratory of Ultra-precision Machining Technology.

Data availability The data obtained in this study are available from the first author on reasonable request.

Declarations

Competing interests The authors declare no competing interests.

References

1. Song YM, Xie Y, Malyarchuk V, Xiao J, Jung I, Choi K-J, Liu Z, Park H, Lu C, Kim R-H, Li R, Crozier KB, Huang Y, Rogers JA (2013) Digital cameras with designs inspired by the arthropod eye. Nature 497:95–99. https://doi.org/10.1038/nature12083
2. Dai B, Jiao Z, Zheng L, Bachman H, Fu Y, Wan X, Zhang Y, Huang Y, Han X, Zhao C, Huang TJ, Zhuang S, Zhang D (2019) Colour compound lenses for a portable fluorescence microscope. Light Sci Appl 8:75. https://doi.org/10.1038/s41377-019-0187-1
3. Buckley E (2010) Holographic projector using one lens. Opt Lett 35:3399. https://doi.org/10.1364/OL.35.003399
4. Itoh Y, Langlotz T, Zollmann S, Iwai D, Kiyoshi K, Amano T (2021) Computational phase-modulated eyeglasses. IEEE Trans Vis Comput Graph 27:1916–1928. https://doi.org/10.1109/TVCG.2019.2947038
5. Dhawan AP, D'Alessandro B, Fu X (2010) Optical imaging modalities for biomedical applications. IEEE Rev Biomed Eng 3:69–92. https://doi.org/10.1109/RBME.2010.2081975
6. Peddie J (2023) Historical overview: ghosts to real AR to DARPA. In: Peddie J (ed) Augmented Reality. Springer International Publishing, Cham, pp 101–133
7. Kumar S, Tong Z, Jiang X (2022) Advances in the design and manufacturing of novel freeform optics. Int J Extrem Manuf 4:32004. https://doi.org/10.1088/2631-7990/ac7617
8. Huang W, Yan J (2023) Effect of tool geometry on ultraprecision machining of soft-brittle materials: a comprehensive review. Int J Extrem Manuf 5:12003. https://doi.org/10.1088/2631-7990/acab3f
9. Yu S, Yao P, Xu J, Wang W, Li Y, Chu D, Qu S, Huang C (2023) Profile error compensation in ultra-precision grinding of aspherical-cylindrical lens array based on the real-time profile of wheel and normal residual error. J Mater Process Technol 312:117849. https://doi.org/10.1016/j.jmatprotec.2022.117849
10. Kakinuma Y, Konuma Y, Fukuta M, Tanaka K (2019) Ultra-precision grinding of optical glass lenses with La-doped CeO2 slurry. CIRP Ann 68:345–348. https://doi.org/10.1016/j.cirp.2019.04.089
11. Lee E-S, Baek S-Y (2007) A study on optimum grinding factors for aspheric convex surface micro-lens using design of experiments. Int J Mach Tools Manuf 47:509–520. https://doi.org/10.1016/j.ijmachtools.2006.06.007
12. Yan G, Zhang Y, You K, Li Z, Yuan Y, Fang F (2019) Off-spindle-axis spiral grinding of aspheric microlens array mold inserts. Opt Express 27:10873–10889. https://doi.org/10.1364/OE.27.010873
13. Yu S, Yao P, Ye Z, Wang W, Chu D, Qu S, Huang C (2022) Simulation and experimental research of tool path planning on profile and surface generation of aspherical-cylindrical lens array by ultra-precision envelope grinding. J Mater Process Technol 307:117690. https://doi.org/10.1016/j.jmatprotec.2022.117690
14. Yu S, Zhu J, Yao P, Huang C (2021) Profile error compensation in precision grinding of ellipsoid optical surface. Chinese J Aeronaut 34:115–123. https://doi.org/10.1016/j.cja.2020.08.042
15. Zhu J, Yao P, Wang W, Huang C, Zhu H, Zou B, Liu H (2019) A helical interpolation precision truing and error compensation for arc-shaped diamond grinding wheel. Int J Adv Manuf Technol 100:167–177. https://doi.org/10.1007/s00170-018-2716-0
16. Liang Y, Cui Z, Zhang C, Meng F, Ma Z, Li M, Yu T, Zhao J (2023) Large size optical glass lens polishing based on ultrasonic vibration. Ceram Int 49:14377–14388. https://doi.org/10.1016/j.ceramint.2023.01.026
17. Zhu W-L, Beaucamp A (2020) Compliant grinding and polishing: a review. Int J Mach Tools Manuf 158:103634. https://doi.org/10.1016/j.ijmachtools.2020.103634
18. Xie W, Zhang Z, Yu S, Li L, Cui X, Gu Q, Wang Z (2023) High efficiency chemical mechanical polishing for silicon wafers using a developed slurry. Surfaces and Interfaces 38:102833. https://doi.org/10.1016/j.surfin.2023.102833
19. Suzuki H, Hamada S, Okino T, Kondo M, Yamagata Y, Higuchi T (2010) Ultraprecision finishing of micro-aspheric surface by ultrasonic two-axis vibration assisted polishing. CIRP Ann 59:347–350. https://doi.org/10.1016/j.cirp.2010.03.117
20. Guo J, Morita S, Hara M, Yamagata Y, Higuchi T (2012) Ultra-precision finishing of micro-aspheric mold using a magneto-strictive vibrating polisher. CIRP Ann 61:371–374. https://doi.org/10.1016/j.cirp.2012.03.141
21. Guo J, Suzuki H, Morita S, Yamagata Y, Higuchi T (2013) A real-time polishing force control system for ultraprecision finishing of micro-optics. Precis Eng 37:787–792. https://doi.org/10.1016/j.precisioneng.2013.01.014
22. Cheung CF, Kong LB, Ho LT, To S (2011) Modelling and simulation of structure surface generation using computer controlled ultra-precision polishing. Precis Eng 35:574–590. https://doi.org/10.1016/j.precisioneng.2011.04.001
23. Hocheng H, Hsieh ML (2004) Signal analysis of surface roughness in diamond turning of lens molds. Int J Mach Tools Manuf 44:1607–1618. https://doi.org/10.1016/j.ijmachtools.2004.06.003
24. Zhang X, Huang R, Liu K, Kumar AS, Shan X (2018) Rotating-tool diamond turning of Fresnel lenses on a roller mold for manufacturing of functional optical film. Precis Eng 51:445–457. https://doi.org/10.1016/j.precisioneng.2017.09.016
25. Du H, Yin T, Li D, Wang Z, Zhu Z, To S (2022) Nanostructure machining and its application in surface information. Surfaces and Interfaces 33:102263. https://doi.org/10.1016/j.surfin.2022.102263
26. Du H, Yip W, Zhu Z, To S (2021) Development of a two-degree-of-freedom vibration generator for fabricating optical microstructure arrays. Opt Express 29:25903. https://doi.org/10.1364/oe.433720
27. Fang F-Z, Huang K-T, Gong H, Li Z-J (2014) Study on the optical reflection characteristics of surface micro-morphology generated by ultra-precision diamond turning. Opt Lasers Eng 62:46–56. https://doi.org/10.1016/j.optlaseng.2014.04.017
28. Chen Y, Li L, Yi AY (2007) Fabrication of precision 3D microstructures by use of a combination of ultraprecision diamond turning and reactive ion etching process. J Micromechanics Microengineering 17:883–890. https://doi.org/10.1088/0960-1317/17/5/006
29. Mukaida M, Yan J (2017) Ductile machining of single-crystal silicon for microlens arrays by ultraprecision diamond turning using a slow tool servo. Int J Mach Tools Manuf 115:2–14. https://doi.org/10.1016/j.ijmachtools.2016.11.004

30. Li P, Wang S, To S, Sun Z, Jiao J, Xu S (2023) High-efficient fabrication of infrared optics with uniform microstructures by a semi-ductile diamond milling approach. Int J Adv Manuf Technol 126:919–934. https://doi.org/10.1007/s00170-023-11140-7
31. Zhang G, Huo Z, Han J, Zhang W, Zheng J (2023) Cutting depth-oriented surface morphology control in diamond-turning brittle single-crystal germanium. J Mater Process Technol 319:118076. https://doi.org/10.1016/j.jmatprotec.2023.118076
32. Zare A, Tunesi M, Harriman TA, Troutman JR, Davies MA, Lucca DA (2023) Face turning of single crystal (111)Ge: cutting mechanics and surface/subsurface characteristics. J Manuf Sci Eng 145. https://doi.org/10.1115/1.4057054
33. Liu G, Kuang D, Song L, Xu C, Yan C (2023) Mechanism in damage variation of nanosecond laser-induced damage of germanium sheets in vacuum. Opt Laser Technol 157:108663. https://doi.org/10.1016/j.optlastec.2022.108663
34. Diener K, Gernandt L, Moeglin J-P, Ambs P (2005) Study of the influence of the Nd:YAG laser irradiation at 1.3µm on the thermal–mechanical–optical parameters of germanium. Opt Lasers Eng 43:1179–1192. https://doi.org/10.1016/j.optlaseng.2004.12.008
35. Du H, Chen H, Zhu Z, Wang Z, To S (2023) Novel hybrid machining process of titanium alloy for texturing high-quality microstructure array surfaces. Surf Coatings Technol 462:129494. https://doi.org/10.1016/j.surfcoat.2023.129494
36. Liu Y-T, Chang W-C, Yamagata Y (2010) A study on optimal compensation cutting for an aspheric surface using the Taguchi method. CIRP J Manuf Sci Technol 3:40–48. https://doi.org/10.1016/j.cirpj.2010.03.001
37. Yin ZQ, Dai YF, Li SY, Guan CL, Tie GP (2011) Fabrication of off-axis aspheric surfaces using a slow tool servo. Int J Mach Tools Manuf 51:404–410. https://doi.org/10.1016/J.IJMACHTOOLS.2011.01.008
38. Yan J, Asami T, Harada H, Kuriyagawa T (2009) Fundamental investigation of subsurface damage in single crystalline silicon caused by diamond machining. Precis Eng 33:378–386. https://doi.org/10.1016/j.precisioneng.2008.10.008
39. Zhang J, Zhang J, Cui T, Hao Z, Al Zahrani A (2017) Sculpturing of single crystal silicon microstructures by elliptical vibration cutting. J Manuf Process 29:389–398. https://doi.org/10.1016/j.jmapro.2017.09.003
40. Wang K, Liu S, Chen F, Liu Z, Luo X (2009) Effect of manufacturing defects on optical performance of discontinuous freeform lenses. Opt Express 17:5457. https://doi.org/10.1364/OE.17.005457
41. Tsai K-M, Hsieh C-Y, Lo W-C (2009) A study of the effects of process parameters for injection molding on surface quality of optical lenses. J Mater Process Technol 209:3469–3477. https://doi.org/10.1016/j.jmatprotec.2008.08.006
42. Zhenkun L, Quan W, Wei Q (2013) Micromechanics of fiber–crack interaction studied by micro-Raman spectroscopy: bridging fiber. Opt Lasers Eng 51:358–363. https://doi.org/10.1016/j.optlaseng.2012.12.003
43. Du H, Kang Y, Xu C, Xue T, Qiu W, Xie H (2022) Measurement and characterization of interfacial mechanical properties of graphene/MoS2 heterostructure by Raman and photoluminescence (PL) spectroscopy. Opt Lasers Eng 149:106825. https://doi.org/10.1016/j.optlaseng.2021.106825
44. Fournier-Lupien J-H, Mukherjee S, Wirths S, Pippel E, Hayazawa N, Mussler G, Hartmann JM, Desjardins P, Buca D, Moutanabbir O (2013) Strain and composition effects on Raman vibrational modes of silicon-germanium-tin ternary alloys. Appl Phys Lett 103:263103. https://doi.org/10.1063/1.4855436
45. Yang Y, Zhan L, Liu C, Xu Y, Li G, Wu X, Huang M, Hu Z (2021) Tension-compression asymmetry of stress-relaxation ageing behavior of AA2219 alloy over a wide range of stress levels. Mater Sci Eng A 823:141730. https://doi.org/10.1016/j.msea.2021.141730
46. Chen X, Zhan L, Ma Z, Xu Y, Zheng Q, Cai Y (2020) Study on tensile/compressive asymmetry in creep ageing behavior of Al–Cu alloy under different stress levels. J Alloys Compd 843:156157. https://doi.org/10.1016/j.jallcom.2020.156157
47. Gao Y, Yang W, Huang Z, Lu Z (2021) Effects of residual stress and surface roughness on the fatigue life of nickel aluminium bronze alloy under laser shock peening. Eng Fract Mech 244:107524. https://doi.org/10.1016/j.engfracmech.2021.107524